Proceedings of ISFOG 2025
5TH INTERNATIONAL SYMPOSIUM ON
FRONTIERS IN OFFSHORE GEOTECHNICS
Nantes, France | June 9-13 2025

ISBN 978-2-85782-758-0

Examining the rate dependency behaviour of sands using DEM simulations

K. Li
China Institute of Water Resources and Hydropower Research, Beijing, China
J. Hu, G. Deng, Z.-T. Zhang*, X.-D. Zhang and Z. Zhang
China Institute of Water Resources and Hydropower Research, Beijing, China
**zhangzt@iwhr.com (corresponding author)*

ABSTRACT: Foundations supporting fixed wind turbines and platforms, such as monopiles in sandy soils, often exhibit the accumulation of permanent deformation over their extended operational lifespan. This behaviour is commonly associated with soil deformation resulting from numerous loading cycles induced by wind and wave loads, as well as the time-dependent characteristics of sands, specifically creep behaviour. Nevertheless, the underlying mechanisms remain inadequately understood. To investigate these mechanisms, this study employs a series of simulations of triaxial tests utilizing the discrete element method. A novel contact model based on the effects of microfracturing of asperities was proposed to capture the time-dependent behaviour. The simulation results show that the stress-strain relationships of the samples under different loading rates exhibited significant differences, which were consistent with the physical experimental results. The outcomes of these DEM simulations enhance our comprehension of the rate dependency of sands. The methodology employed in this study can be extrapolated to other scenarios where sands are subjected to intricate loading-unloading histories, with creep playing a crucial role that cannot be overlooked.

Keywords: Creep; Strain rate; DEM; Microfracturing; Sensitivity analysis

1 INTRODUCTION

The development of offshore wind power projects toward deeper and more remote sea areas imposes higher requirements for ensuring safety and stability of the associated structures during operation. The foundations of offshore wind turbines, e.g, monopiles, may experience permanent deformations over service periods due to the coupling effects of lateral loading and time-dependent behaviour. Chegenizadeh et al. (2020) conducted triaxial tests with constant strain rates on silty sand with a mean diameter d_{50} of 0.035 mm, revealing that strain rate significantly influences both the stress-strain and volumetric behaviour. When the strain rate decreased from 1.19×10^{-4}/s to 1.19×10^{-7}/s, the deviatoric stress and volumetric strain corresponding to the same axial strain could reduce to 50% of their original values, suggesting significant rate-dependency.

Similarly, the creep behaviour under zero loading rate is also highly influenced by the pre-loading rate. Karimpour et al. (2013) conducted creep tests on Virginia Beach sand with a size of 0.425 mm ~ 0.850 mm after loading at various rates. The results showed that the creep rates of axial and volumetric strains increased with increasing pre-loading rates, with significant differences in strain values at the same creep time. The creep strain values at 100 - 1000 min with a relatively high pre-loading rate (1.1×10^{-4}/s) reached 2~3 times those observed with a relatively low strain rate (4.3×10^{-7}/s).

Matsushita et al. (1999) conducted CD-TC tests on Toyoura sand with a mean diameter d_{50} of 0.18 mm to study the stress-strain behaviour during changing loading strain rates. The results demonstrated that when the loading strain rate increased abruptly, the specimen exhibited highly rigid, nearly elastic characteristics. Following this sudden increase, with further strain accumulation, the specimen showed a marked yield point and then the stress-strain curve becomes close to the curve with a relatively low strain rate.

Those experimental results clearly indicate the interaction between loading and time-dependent behaviour. This study aims to propose a robust and efficient numerical model to consider those coupling effects of loading and creep on the mechanical behaviour of soils. The micromechanics of creep are firstly summarized, and the numerical model is then introduced. After that, the numerical results of triaxial compression tests with various strain rates are discussed to verify the capacity of the proposed method.

2 CREEP MECHANISMS

Initially, some researchers attributed creep behaviour to chemical and biological changes between particles (e.g., Mitchell, 1986); however, creep behaviour has also been observed in clean dry sand (Mesri et al., 1990). With advances in related theories, some scholars have suggested

that creep behaviour in sandy soils is associated with particle rearrangement (e.g., Wang et al., 2008), driven by the formation of micro-cracks on particle surfaces.

Lade et al. (2009, 2010a, 2010b) conducted a series of triaxial creep and relaxation tests, attributing the observed creep behaviour in sand to quasi-static particle breakage. Brzesowsky et al. (2014) carried out 1D secondary compression tests and inferred that time-dependent deformation is driven by subcritical crack growth, which initiates particle breakage, sliding, and rearrangement as a result of subcritical crack propagation. Although these experimental observations on particle breakage were obtained with relatively brittle sands, the very small contact areas between particles lead to high interparticle contact stresses. Therefore, even stronger siliceous sands may develop micro-cracks or break at contact points under low stress states.

Frictional dynamics research indicates that at the onset of sliding, fracture-like or crack-like fronts (similar to these micro-cracks) rapidly form, causing the contact surface to transition from a stick to a slip state (Rubinstein, 2004). Consequently, the formation of micro-cracks or fractures between particles reduces interparticle contact forces, leading to relative sliding and a forced rearrangement of the entire particle system toward equilibrium. With increased loading, the formation of new cracks initiates this process anew, suggesting that the entire creep behaviour can be understood as a series of these cycles (Zhang and Wang, 2016).

3 SIMULATION METHODS

This study utilizes the DEM software Particle Flow Code in three dimensions to conduct numerical simulation tests on sand creep behaviour. The contact model, parameters and test program will be presented in the following.

3.1 Contact model

The approach proposed by Zhang and Wang (2016) was modified to capture the time-dependent behaviour of soils. The generation of microcracks or breakage on particle surfaces is represented by reducing the resultant contact force. This process is modeled in the program using two parameters: the attenuation coefficient α and the attenuation interval λ. As illustrated in Figure 1, the contact force at time t, is F. After a time interval Δt, the formation of microcracks or breakage on particle surfaces reduces the contact force between particles to αF, resulting in relative sliding between particles. This induces a redistribution of contact forces, with the adjusted force becoming F'. The time intervals between successive adjustments are kept constant and are controlled in the program using the attenuation interval λ. The value of λ represents the number of cycles required for the force attenuation to progress from the N^{th} to the $(N+1)^{th}$ step. To ensure consistent time intervals, the timestep is fixed at 1×10^{-7} s. Furthermore, the parameters α and λ remain unchanged across tests conducted at different loading rates.

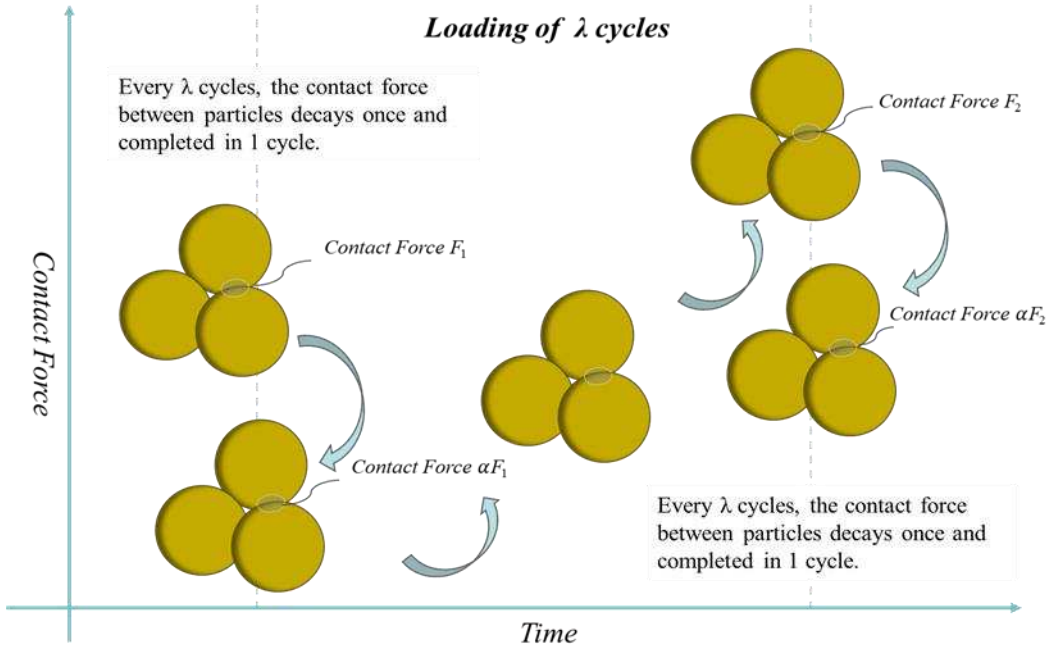

Figure 1– Schematic diagram showing how the contact force between particles decays and readjusts to a new equilibrium state

In addition, the Edinburgh-Elasto-Plastic-Adhesive (EEPA) model was used to capture the elasto-plastic behaviour of soils. The EEPA model is an extension of the linear hysteretic model, which allows for the generation of tensile forces between particles and accounts for nonlinear behaviour during compression. It also incorporates viscous damping and rolling resistance. Specifically, this model describes the elasto-plastic deformation of the system through nonlinear equivalent hysteretic springs, provides cohesive forces for plastic contact deformation, and captures the history-dependent behaviour. The parameters used in the model are shown in Table 1.

3.2 Simulation program

As indicated in Table 2, there were in total 12 test carried out in this study. The contact model proposed in this study was employed in Tests 1 through 10, while the EEPA model was utilized in Tests 11 to 13. Samples 1 and 2 have different loading rates but identical creep parameters. Samples 2 ~ 6 are tested with the same loading rate and attenuation coefficient α, but different attenuation intervals λ. Samples 2 and 7 ~ 10 are tested with the same loading rate and attenuation interval λ, but different attenuation coefficients α. In the simulations, the parameter α ranges from 0.99 to 0.999, while the values of λ vary between 20,000 and 200,000. In each simulation, after preloading all samples under isotropic compression of 200 kPa, an axial load was applied at a specified rate until a 10% axial strain was achieved.

Table 1. Sample properties and contact model parameters adopted in the DEM simulations of this study

Sample properties and parameters	Value
Sample sizes (mm)	2.12×2.12×4.14
Particle sizes (mm)	0.212
Contact model parameters	
Shear modulus G (GPa)	1.43
Poisson's ratio ν	0.3
Sliding friction coefficient μ	0.4
Pull-off force F^0	0
Rolling friction coefficient μ_r	1.2
Normal critical damping ratio β_n	0.2
Shear critical damping ratio β_s	0.2
Shear critical damping ratio M_d	0
Time step	1×10^{-7} s

4 RESULTS

4.1 Verification of the proposed model

The results from tests 11 to 13 are firstly examined. Figures 2 and 3 present the stress-strain and the volumetric strain-axial strain curves, respectively, under conditions where creep effects are not considered. It can be observed that, for the experiments conducted in this study, an increase in the loading rate leads to an increase in both the deviatoric stress of the specimens at lower strain levels and volumetric deformation of the specimens. This finding is consistent with the results reported in previous experimental studies. When the loading rate is reduced to 2.07×10^{-4} m/s or lower, the resulting stress-strain curves are observed to almost completely overlap when creep effects are neglected, indicating that the influence of strain rate becomes negligible in this scenario. Therefore, in this study, 2.07×10^{-4} m/s is considered the critical value for the quasi-static loading rate.

Table 2. Arrangement of the DEM simulations for triaxial creep

No.	Loading rate (m/s)	Attenuation coefficient α	Attenuation interval λ	Isotropic compression pressure (kPa)	Remarks
1	$10V_0$	0.999	20000	200	Model proposed in this study
2	V_0	0.999	20000	200	Model proposed in this study
3	$10V_0$	0.999	200000	200	Model proposed in this study
4	$10V_0$	0.999	100000	200	Model proposed in this study
5	$10V_0$	0.999	10000	200	Model proposed in this study
6	$10V_0$	0.999	5000	200	Model proposed in this study
7	$10V_0$	0.9999	20000	200	Model proposed in this study
8	$10V_0$	0.9995	20000	200	Model proposed in this study
9	$10V_0$	0.995	20000	200	Model proposed in this study
10	$10V_0$	0.99	20000	200	Model proposed in this study
11	$100V_0$	/	/	200	EEPA model
12	$10V_0$	/	/	200	EEPA model
13	V_0	/	/	200	EEPA model

$V_0 = 2.07\times10^{-5}$ m/s.

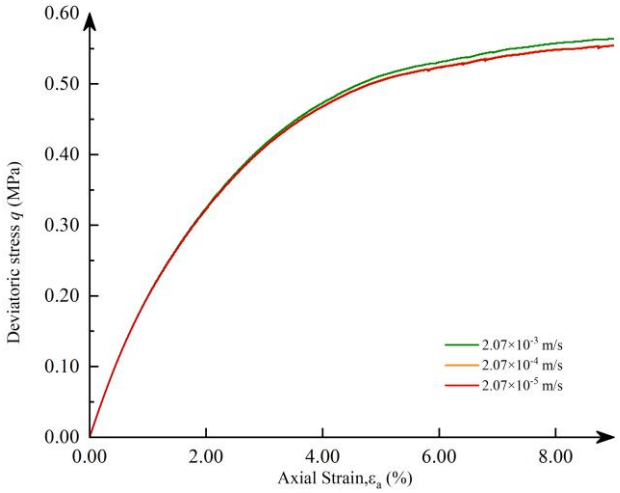

Figure 2– The stress-strain responses of simulation results of triaxial without creep at V_0, $10V_0$.

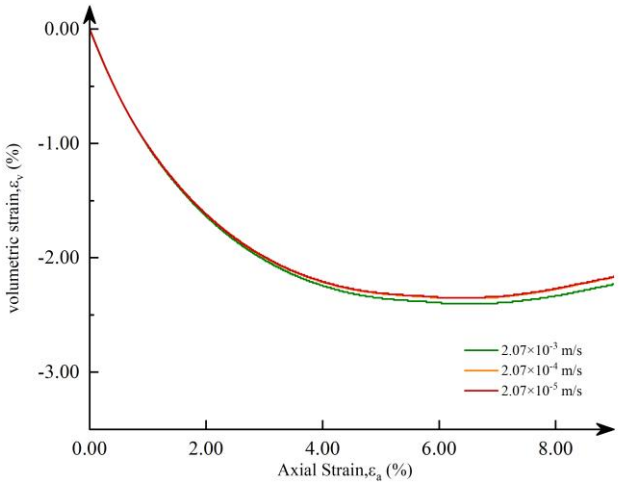

Figure 3– The stress-strain responses of simulation results of triaxial without creep at V_0, $10V_0$.

Figures 4 and 5 document the stress-strain curves and volumetric strain-axial strain relationships, respectively, under different loading rates with creep effects considered in tests 1 and 2. It can be observed that the stress-strain curves under different loading rates initially overlap at lower strain levels, gradually diverge as strain increases, and reach their maximum difference at approximately 4% strain before converging again at higher strain levels. Notably, no distinct yield point is evident. At higher strain rates, specimens tend to exhibit greater strength at lower strains and demonstrate more pronounced linear elastic behavior. However, the it has no significant effect on the peak stress.

The volumetric strain shows a decreasing trend with increasing strain rates, and the specimens clearly exhibit initial contraction followed by dilation during loading. These findings are consistent with the experimental results reported by Yamamuro et al. (2011). Compared to the results without considering creep effects, the stress-strain and volumetric strain-axial strain curves of specimens with creep effects already display noticeable differences at very low strains under different strain rates.

This indicates that creep effects are the primary reason why strain rates influence the stress-strain behaviour of sand under low strain rates. In addition, creep effects significantly enhance the sensitivity of stress-strain and volumetric strain-axial strain relationships to strain rate variations at low strain rates.

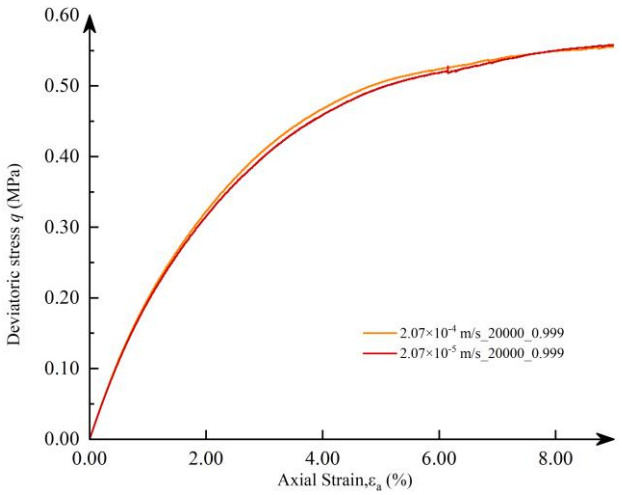

Figure 4– The stress-strain responses of simulation results of triaxial with creep at V_0, $10V_0$.

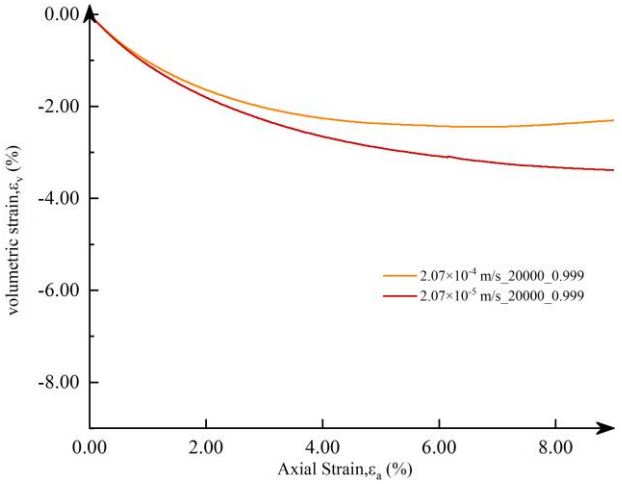

Figure 5– The volumetric responses of simulation results of triaxial with creep at V_0, $10V_0$.

4.2 Sensitivity to parameter λ

This study primarily uses two parameters, the attenuation coefficient α and the attenuation interval λ, to describe the creep behaviour in the samples. The coefficient α is used to represent the extent of particle breakage in the sample, with a larger α indicating lower particle breakage. On the other hand, λ is inversely related to the number of times the particle breakage process occurs, which is necessary for inducing particle rearrangement within the entire system. In other words, a larger value of λ corresponds to fewer occurrences of particle rearrangement.

During the sensitivity analysis, experiments were conducted with various combinations of α and λ (see Table 2). The results of these parameter combinations are presented below, and their impact on the creep behaviour of sand is analyzed.

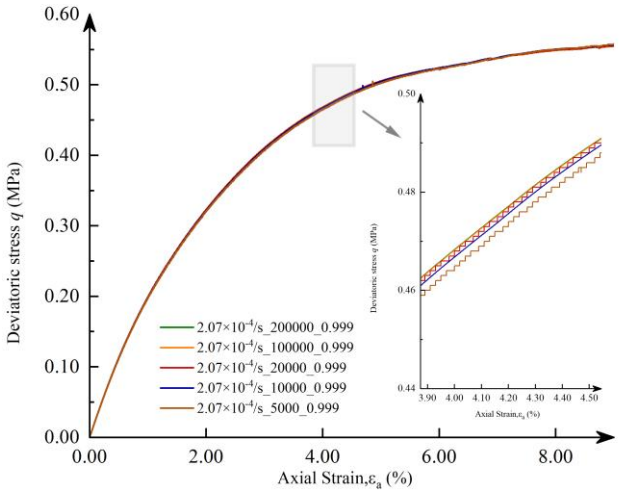

Figure 6– The stress-strain responses of simulation results of triaxial creep at $10V_0$ for different attenuation interval λ.

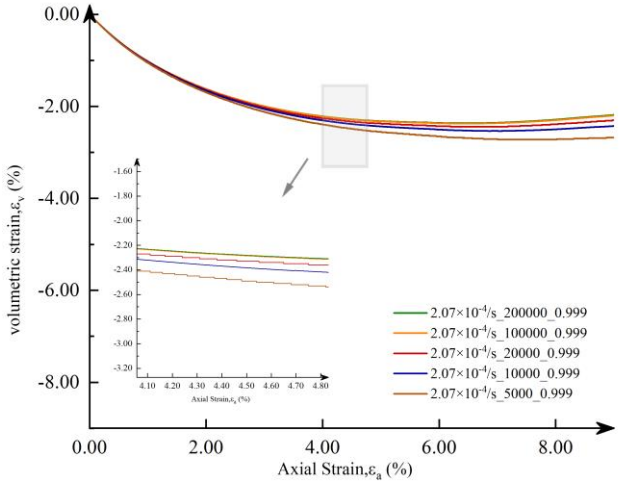

Figure 7– The volumetric responses of simulation results of triaxial creep at $10V_0$ for different attenuation interval λ.

Figures 6 and 7 illustrate the experimental results for samples 2 ~ 6. As shown in Figure 6, when the value of α is fixed, the deviatoric stress of the specimens at lower strain levels generally increases with larger λ values. From Figure 7, it can be observed that in the volumetric strain-axial strain relationship, volumetric deformation decreases as λ increases.

These findings indicate that an increase in λ results in higher deviatoric stress of the specimens at lower strain levels and reduced volumetric strain, with the changes in volumetric strain becoming more pronounced. However, when λ exceeds a certain threshold, further increases in its value have negligible effects on the results. Conversely, when λ is below this threshold, the volumetric strain of the specimens increases significantly, although similar behaviour is not observed in the stress-strain relationship.

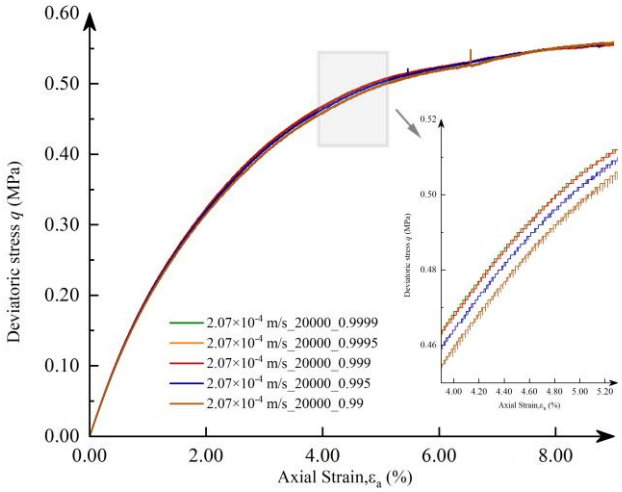

Figure 8– The stress-strain responses of simulation results of triaxial creep at $10V_0$ for different attenuation coefficient α.

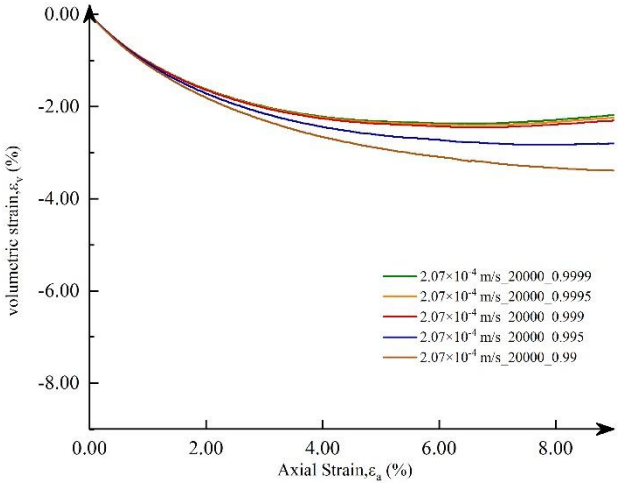

Figure 9– The volumetric responses of simulation results of triaxial creep at $10V_0$ for different attenuation coefficient α.

4.3 Sensitivity to parameter α

Figures 8 and 9 display the experimental results for samples 2 and 7 ~10. As shown in Figure 6, when λ is fixed, the deviatoric stress of the specimens at lower strain levels generally increases with higher α values. From Figure 7, it can be observed that in the volumetric strain-axial strain relationship, volumetric deformation decreases as α increases.

These results indicate that increasing α leads to higher deviatoric stress of the specimens at lower strain levels and reduced volumetric strain, with the changes in volumetric strain becoming more pronounced. However, when α exceeds a certain threshold, further increases have minimal effects on the results. Conversely, when α is below this threshold, the volumetric strain increases significantly, while no similar trend is observed in the stress-strain relationship. This behaviour is consistent with the trends observed when adjusting λ; however, the results are evidently more sensitive to changes in α.

5 CONCLUSION

A novel contact model has been proposed to simulate the time-dependent behaviour of sands. This model is grounded in a solid physical framework and comprises only two parameters, facilitating straightforward calibration. A series of discrete element method (DEM) simulations were conducted to perform a sensitivity analysis of these parameters. The results indicate that increases in λ and/or α lead to higher deviatoric stress of the specimens at lower strain levels and reduced volumetric strain, with the changes in volumetric strain becoming increasingly pronounced. The sensitivity analysis of the creep parameters demonstrates that once these parameters reach a certain threshold, further modifications have a minimal impact on the stress-strain and volumetric strain-axial strain relationships of the samples. Notably, the attenuation coefficient α exerts a more significant influence on these relationships than the other parameter. While the model exhibits considerable potential, additional physical tests and numerical simulations are necessary to further validate the proposed framework.

AUTHOR CONTRIBUTION STATEMENT

Ke Li: Data curation, Software, Writing-Original draft. **Jing Hu**: Visualization, Investigation. **Gang Deng**: Supervision, Funding acquisition. **Zitao Zhang**: Software, Conceptualization, Methodology, Supervision, Writing- Reviewing and Editing. **Xuedong Zhang**: Conceptualization, Methodology, Supervision. **Zheng Zhang**: Software, Conceptualization, Methodology.

REFERENCES

Brzesowsky, R., Hangx, S., Brantut, N., Spiers, C. (2014) Compaction creep of sands due to time-dependent grain failure: effects of chemical environment, applied stress, and grain size, *Journal of Geophysical Research*, 119(10), pp. 7521-7541, https://doi.org/10.1002/2014JB011277

Chegenizadeh, A., Keramatikerman, M., Nikraz, H. (2020) Effect of loading strain rate on creep and stress-relaxation characteristics of sandy silt, Results in Engineering, Volume (7), pp. 100143, https://doi.org/10.1016/j.rineng.2020.100143

Karimpour, H., Lade, P. V. (2013) Creep behaviour in Virginia Beach sand, Canadian Geotechnical Journal, 50(11), pp. 1159-1178, http://doi.org/10.1139/cgj-2012-0467

Lade, P. V., Karimpour, H. (2010) Static Fatigue Controls Particle Crushing and Time Effects in Granular Materials, *Soils and Foundations*, 50(5), pp. 573-583, https://doi.org/10.3208/sandf.50.573

Lade, P. V., Liggio, C. D., Nam, J. (2009) Strain rate, creep and stress drop-creep experiments on crushed coral sand, *Journal of Geotechnical and Geoenvironmental Engineering*, 135(7), pp. 941-953, https://doi.org/10.1061/(ASCE)GT.1943-5606.0000067

Lade, P. V., Nam, J., Liggio, C. D. (2010) Effects of particle crushing in stress drop-relaxation experiments on crushed coral sand, *Journal of Geotechnical and Geoenvironmental Engineering*, 136(3), pp. 500-509, https://doi.org/10.1061/(ASCE)GT.1943-5606.0000212

Matsushita, M., Tatsuoka, F., Koseki, J., Cazacliu, B., Benedetto, H., Yasin, SJM. (1999) Time effects on the pre-peak deformation properties of sands, In: Pre-failure deformation characteristics of geomaterials, Turin, Italy, pp. 681-689.

Mesri, G., Feng, T. W., Benak, J. M. (1990) Postdensification Penetration Resistance of Clean Sands, *Journal of Geotechnical and Geoenvironmental Engineering*, 116(7), pp. 1095-1115, https://doi.org/10.1061/10.1061/(ASCE)0733-9410(1990)116:7(1095)

Mitchell, J. K. (1986) Practical problems from surprising soil behaviour, *Journal of Geotechnical Engineering*, 112(3), pp. 259-289, https://doi.org/10.1061/(ASCE)0733-9410(1986)112:3(255)

Rubinstein, S., Cohen, G., Fineberg, J. (2004) Detachment fronts and the onset of dynamic friction, *Nature*, **430**, pp. 1005-1009, https://doi.org/10.1038/nature02830

Wang, Y. H., Xu, D., and Tsui, K. Y. (2008) Discrete element modeling of contact creep and aging in sand, *Journal of Geotechnical and Geoenvironmental Engineering*, 134(9), pp. 1407-1411, https://doi.org/10.1061/(ASCE)1090-0241(2008)134:9(1407)

Yamamuro, J. A., Abrantes, A. E., Lade, P. V. (2011) Effect of strain rate on the stress-strain behaviour of sand, *Journal of Geotechnical and Geoenvironmental Engineering*, 137(12), pp. 1169-1178, https://doi.org/10.1061/(ASCE)GT.1943-5606.0000542

Zhang, Z. T., Wang, Y. H. (2016), modeling of aging or creep in sand based on the effects of microfracturing of asperities and evolution of microstructural anisotropy during triaxial creep, *Acta Geotechnica*, 11(6), pp. 1303-1320, https://doi.org/10.1007/s11440-016-0483-3